



tert-butoxides as precursors for atomic layer deposition of alkali metal containing thin films


Cite as: J. Vac. Sci. Technol. A **38**, 060804 (2020); <https://doi.org/10.1116/6.0000589>

Submitted: 28 August 2020 . Accepted: 01 October 2020 . Published Online: 20 October 2020

 Henrik H. Sønsteby, Jon E. Bratvold, Veronica A.-L. K. Killi, Devika Choudhury, Jeffrey W. Elam, Helmer Fjellvåg, and  Ola Nilsen

COLLECTIONS

Paper published as part of the special topic on [Atomic Layer Deposition \(ALD\) ALD2021](#)

 This paper was selected as Featured



View Online



Export Citation



CrossMark

ARTICLES YOU MAY BE INTERESTED IN

[Consistency and reproducibility in atomic layer deposition](#)

Journal of Vacuum Science & Technology A **38**, 020804 (2020); <https://doi.org/10.1116/1.5140603>

[Ultrasonic atomization of titanium isopropoxide at room temperature for TiO₂ atomic layer deposition](#)

Journal of Vacuum Science & Technology A **38**, 062405 (2020); <https://doi.org/10.1116/6.0000464>

[Conformality in atomic layer deposition: Current status overview of analysis and modelling](#)
Applied Physics Reviews **6**, 021302 (2019); <https://doi.org/10.1063/1.5060967>



Advance your science and
career as a member of

AVS

LEARN MORE




tert-butoxides as precursors for atomic layer deposition of alkali metal containing thin films

Cite as: J. Vac. Sci. Technol. A 38, 060804 (2020); doi: 10.1116/6.0000589

Submitted: 28 August 2020 · Accepted: 1 October 2020 ·

Published Online: 20 October 2020



Henrik H. Sønsteby,^{1,2,a)}  Jon E. Bratvold,¹ Veronica A.-L. K. Killi,¹ Devika Choudhury,² Jeffrey W. Elam,^{2,3} Helmer Fjellvåg,¹ and Ola Nilsen^{1,b)} 

AFFILIATIONS

¹Department of Chemistry, University of Oslo, Blindern, 0315 Oslo, Norway

²Argonne National Laboratory, Argonne, Illinois 60439

³Advanced Materials for Energy-Water Systems (AMEWS) Energy Frontier Research Center (EFRC), Lemont, Illinois 60439

Note: This paper is part of the 2021 Special Topic Collection on Atomic Layer Deposition (ALD).

^{a)}Electronic mail: henrik.sonsteby@kjemi.uio.no

^{b)}Electronic mail: ola.nilsen@kjemi.uio.no

ABSTRACT

Alkali metal containing materials have become increasingly attractive in a world hunting for sustainable energy materials and green functional devices. Lithium- and sodium battery technology, lead-free piezo- and ferroelectric devices, and record-breaking alkali doped tandem perovskite solar cells are among the applications where alkali metal-containing thin films get increasing attention. Atomic layer deposition (ALD) is one of the enabling thin film deposition techniques that offer chemical and geometrical versatility to realize the implementation of such thin films on an applicable scale. The drawback has until recently been a lack of available precursor chemistry that offers self-limiting growth that is fundamental to ALD. The alkali metal *tert*-butoxides have been shown to exhibit the necessary properties to facilitate saturating growth for Li-, Na-, K-, and Rb-containing compounds. However, the behavior of the *tert*-butoxides in ALD-growth has been considered difficult to unravel, with processes exhibiting limited control and low reproducibility. Very little has been reported on trends in reaction mechanisms as the mass of the alkali metal increases. Herein, we summarize the existing literature on the use of alkali metal *tert*-butoxides as precursors in ALD. We consider differences in the structure and behavior of the *tert*-butoxides as the alkali metal cation becomes heavier. In addition, we present precursor synthesis routes and key information on precursor structure, stability, and mechanistic behavior. Finally, we provide the first ever report of Cs-containing films by ALD to complement previous work on its lighter counterparts.

Published under license by AVS. <https://doi.org/10.1116/6.0000589>

I. INTRODUCTION

Our modern society faces enormous challenges that can only be overcome by a strong focus on sustainable development. Clean and green energy is one important issue, ranging from harvesting to storage and effective use. This is, however, only one of many sustainability challenges that the scientific community needs to address in the coming years. As an example; a large part of our high-tech everyday life is based on electronic components that contain toxic heavy metals, most prominently lead (Pb). The use of lead does not only instigate acute toxicity from environmental pollution, but also causes long-term harm to workers in third world lead-producing countries.¹

As a means to shift to more sustainable technologies, there has been a surge in the development of new materials that do not contain harmful, toxic, or geographically limited elements. Within these, alkali metal containing oxides are believed to become central. The most prominent example is lithium in modern batteries and the rise of sodium as a low-cost and long-term sustainable alternative to lithium for large scale batteries.² Solid solutions of *sodium*- and *potassium niobates* ($K_xNa_{1-x}NbO_3$, KNN) and variants thereof are shown to be viable green replacements for the current lead-containing piezo- and ferroelectric workhorse *lead zirconate titanate* (PZT).³ Furthermore, rubidium- and cesium containing tandem perovskite solar cells are breaking efficiency records every year.^{4,5}

The asset of the alkali metals lies in their nontoxicity, in addition to their large natural abundance and availability, especially for sodium and potassium. It has, however, become well known that using alkali metals in the synthesis of inorganic functional materials is challenging. The alkali cations are usually very mobile in the host structure, and their oxides are often volatile at elevated temperatures, causing loss of material and loss of stoichiometric control during traditional synthesis.

A pertinent issue is the deposition of alkali containing complex oxides as *thin films*. Many of the interesting technological applications for alkali metal containing compounds require the materials to be applied as thin coatings. However, the high mobility and volatility of the alkali elements makes it particularly challenging to achieve uniform films and composition control over larger areas using the traditional deposition conditions for sputtering, molecular beam epitaxy (MBE), pulsed laser deposition (PLD), and chemical vapor deposition (CVD). Solution based techniques, such as solgel, can be employed, however, these tend to suffer from chemical pre-reactions and crack formation due to shrinkage during solvent evaporation.

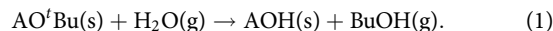
One technique that excels in conformal deposition of alkali metal containing films is atomic layer deposition (ALD). ALD has been successfully used to deposit a wide range of alkali containing materials over the last 10 years. This includes a range of lithium compounds (e.g., LiS, LiNbO₃, and LiCoO₂), but also technologically important compounds with other alkali elements, such as KNN and KTa_{1-x}Nb_xO₃ (KTN), in addition to rubidium-containing compounds.⁶⁻¹⁰ This has for a large part been made possible by the use of alkali metal *tert*-butoxides as ALD-precursors. These precursors are known to enable high conformality and strong compositional control. They offer very clean chemistry, leaving very little carbon contamination in the films.

Not much has been reported, however, on the *growth behavior* and *mechanisms* of alkali metal *tert*-butoxides in ALD. Some detailed descriptions of lithium processes have been made, but general the consensus is that a deeper understanding of *tert*-butoxides in ALD has been quite difficult to acquire. Sonstebly *et al.* recently provided some mechanistic insight for the growth of KNbO₃, highlighting the caveats of alkali metal containing ALD, but a more general understanding has yet to be reported.¹¹

Herein, we summarize all the existing literature on the use of alkali metal *tert*-butoxides as precursors in ALD. We report on facile synthesis techniques for obtaining high-purity *tert*-butoxides for all the alkali metal elements. We treat a wide variety of reports on ALD of Li containing compounds, in addition to an exhaustive, yet smaller set of processes for Na, K, and Rb. We show how the surprising gas phase structure of the precursor molecules can lead to very rapid alkali metal ion incorporation and shed light on the importance of the strong hygroscopicity of intermediary alkali oxide/hydroxide species. We look at differences in growth as the alkali metal becomes heavier, with a clear separation taking place between NaO^tBu and KO^tBu. Finally, we show the first proof-of-concept deposition of Cs-containing films by ALD, using CsO^tBu, which will be increasingly important in developing tandem perovskite photovoltaics.

II. ALKALI METAL *tert*-BUTOXIDES

Alkali metal *tert*-butoxides are described by the general formula AOC(CH₃)₃ (or AO^tBu) and consist of one *tert*-butoxide group per univalent alkaline metal ion. They are strong non-nucleophilic bases (stronger than, e.g., their hydroxide counterparts), but do not take part in nucleophilic addition reactions due to steric hindrances of the central carbon atom. They dissolve easily in tetrahydrofuran (THF) or pentane. Furthermore, they react readily with water, forming the respective hydroxides and *tert*-butanol,



They are all based on deprotonation and bonding to the simplest of tertiary alcohols: *tert*-butanol or *tert*-butyl alcohol (Fig. 1).

It is natural to think that the alkali metal *tert*-butoxides adopt a monomeric structure, with a univalent alkali metal ion bonded to one *tert*-butoxide ligand, and for chemical intuition on reaction products in organic chemistry this view dominates and is likely sufficient. However, it has been shown that these molecules do not adopt monomeric forms in the solid phase nor in the gas phase. They form a variety of stabilizing oligomer clusters, where the number of units vary with the mass of the alkali metal.¹²⁻¹⁵ Lithium- and sodium *tert*-butoxide predominantly adopt a hexamer form (also heptamer, octamer, and nonamer depending on the conditions), whereas the heavier potassium-, rubidium, and cesium *tert*-butoxides predominantly adopt a tetrameric form in a cubanelike base structure (Fig. 2). The oligomer gas phase stability has been shown by mass spectrometry studies, where the larger cluster molecules tend to be the dominating species. Note that these cluster molecules still violently react with water, to form the respective hydroxides and *tert*-butanol. This reaction is highly exothermic, and the resulting *tert*-butanol can spontaneously ignite. The ALD chemist will hopefully find some reassurance knowing that the alkali metals are polycoordinated in the precursor molecule,

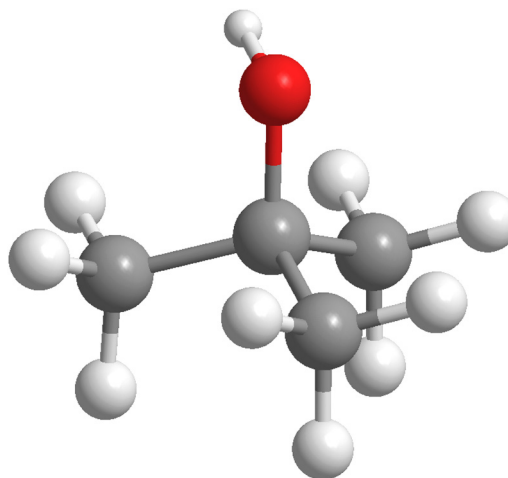


FIG. 1. Ball-and-stick model of the *tert*-butanol or *tert*-butyl alcohol molecule. Gray balls are carbon, red are oxygen, and white are hydrogen.

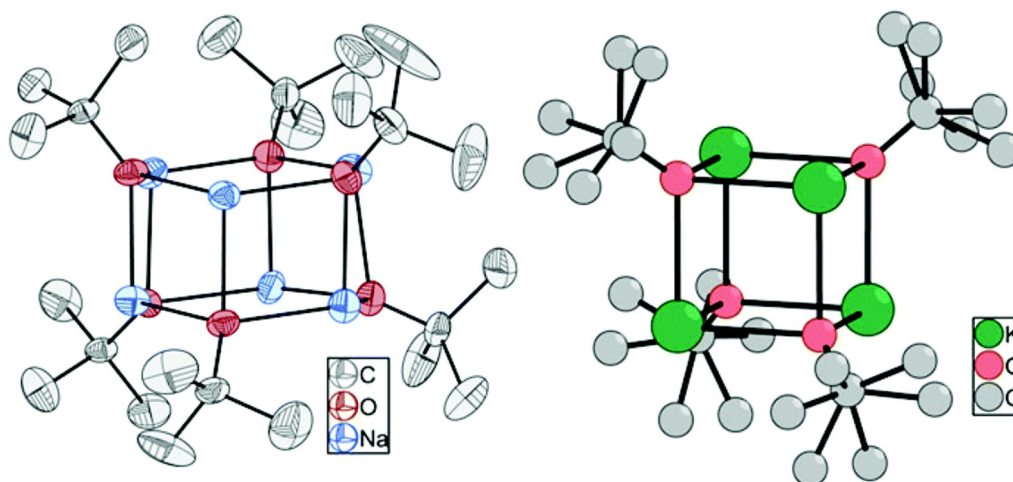


FIG. 2. Sketches of the hexamer structure adopted by lithium- and sodium *tert*-butoxide (exemplified by sodium *tert*-butoxide) and the cubanelike tetramer structure taken by potassium-, rubidium-, and cesium *tert*-butoxide (exemplified by potassium *tert*-butoxide). Reprinted with permission from Østreg *et al.*, *Dalton Trans.* **43**, 16666 (2014). Copyright 2014, Royal Society of Chemistry.

opening for a more stringent discussion on surface reactions and growth behavior.

The vapor pressure of the different *tert*-butoxides depends strongly on the adopted conformer, in addition to the electron affinity and mass of the respective alkali metal. At 0.1 mbar, effective sublimation temperatures for purification are reported to be 110 °C, 140 °C, 150 °C, 190 °C, and 200 °C, for Li-, Na-, K-, Rb-, and CsO^tBu, respectively.^{13,14,16}

Thermogravimetric analysis (TGA) show the same sublimation behavior for all of the compounds in question, with a small mass decrease starting at around 50 °C where crystal *tert*-butanol is released from the [AO^tBu]_x · [Bu^tOH] network, before the oligomer itself starts to sublime (example for RbO^tBu in Fig. 3).¹⁷ This crystal *tert*-butanol is not readily removed during synthesis, but by post-synthesis *in vacuo* re-sublimation either *ex* or *in situ*. The sublimation of the precursor itself is clean and in *one* major step, with a relatively low residual mass, an important quality to look for when selecting precursors for gas-to-solid deposition techniques. Note that the precursor was exposed to air for a short period of time (in the order of seconds) before TGA, and the residual mass might be a result of this exposure. A similar residual mass was also observed for the Na- and K *tert*-butoxides.¹³ Although some of the precursors have a slightly higher sublimation temperature compared to other common precursor compounds, they offer physical properties that make them viable for use in ALD.

One major drawback of the alkali metal *tert*-butoxides, typical for all volatile alkali metal compounds, is the strong hygroscopicity and tendency to degrade upon exposure to humidity [according to Eq. (1)]. While this is not surprising and warrants handling in inert atmosphere, the reactions are not necessarily obvious to the naked eye, and may be easily overlooked. When these compounds are handled in air, they react with humidity and form a transparent gel-like substance that encapsulates the precursor molecules. This is

detrimental to the vapor pressure, as the alkali hydroxides exhibit very limited volatility at typical ALD temperatures. In other words, even if there is very little visual change in the precursor, its sublimation is heavily affected, leading to prolonged pulsing to obtain the required precursor dose (Fig. 4).¹⁸ This may cause serious difficulties in reproducing and replicating previous work, and the only

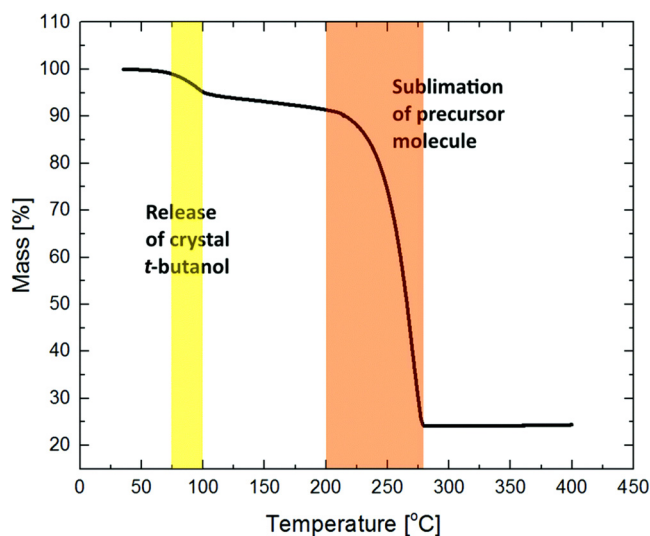


FIG. 3. Thermogravimetric analysis of alkali metal *tert*-butoxides, exemplified by RbO^tBu. The temperature range at which crystal *tert*-butanol is released is marked in yellow (75 – 100 C), whereas the sublimation of RbO^tBu is marked in orange (200 – 277 C). Reproduced with permission from Sønstebj *et al.*, *Dalton Trans.* **46**, 16139 (2017). Copyright 2017, Royal Society of Chemistry.

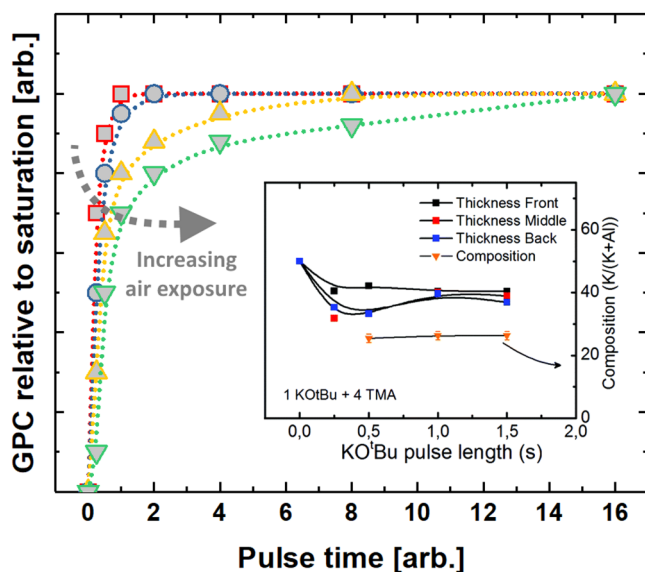


FIG. 4. Theoretical example of pulse times needed to reach saturation as a function of handling time in air for alkali metal *tert*-butoxides. Prolonged air handling time drastically increases pulse time needed for saturation. Change in physical appearance of the precursor is almost unnoticeable in the early stages. Reprinted with permission from Sønsteby *et al.*, *J. Vac. Sci. Technol. A* **38**, 020804 (2020). Copyright 2020, Author(s). Inset: Typical saturation curve for potassium *tert*-butoxide when used together with TMA and water to deposit $K_xAl_yO_z$. Handling time in air was limited to an absolute minimum. The inset reprinted with permission from Østreg *et al.*, *Dalton Trans.* **43**, 16666 (2014). Copyright 2014, Royal Society of Chemistry.

way to avoid these issues is by completely avoiding contact with air and/or moisture. In practice, however, it has been shown that limited exposure to air is tolerable, i.e., filling a vessel for transfer to an ALD reactor. Storing the precursor under inert conditions and only introducing it to air when loading the precursor into the reactor seems to be sufficient for acceptable reproducibility.

A. Synthesis of *tert*-butoxide precursors

The alkali metal *tert*-butoxides can be synthesized using the same, relatively straightforward, route with high yields.¹³ The desired alkali metal is added to an aliquot of dry THF where a stoichiometric amount of *tert*-butanol has been dissolved (1:1), preferably in a round bottom flask. A slight superstoichiometry of *tert*-butanol may be advantageous for complete dissolution of the alkali metal. This *tert*-butanol will remain in the product as crystal *tert*-butanol and should be removed by postsynthesis resublimation before use. Note that *tert*-butanol and alkali metal addition must be carried out under inert atmosphere, preferably in a glove box, and that the THF and *tert*-butanol must be dry to avoid detrimental hydroxide formation. The flask is connected to a Schlenk line or other inert synthesis setup and stirred overnight, or until all visible metal has disappeared. During this step, it may be necessary to heat to reflux to speed up the reaction, depending on the alkali metal. Rb and Cs require very little

added heat due to their low melting points. The solution is filtered and the solvent removed *in vacuo*. The crude product is then resublimed *in vacuo* at a temperature slightly below the reported sublimation temperatures of the clean *tert*-butoxides. The product is a white, moisture sensitive solid, commonly with >90% yield. ¹H NMR for a properly clean product reveals only one strong singlet slightly above δ 1 ppm (Me_3C , 9H), which corresponds to hydrogen in the methyl groups. Li-, Na-, and KO^tBu are commercially available at around \$ 5 g^{-1} , making them very inexpensive as ALD precursors. Storage time inside a dry glove box seems to be in the order of years; however, the bench lifetime is very short due to reaction with moisture and should be limited. Rb- and CsO^tBu are not readily commercially available and must be synthesized in-house. Their cost is governed by the raw metals (Rb: \$ 100 g^{-1} , Cs: \$ 200 g^{-1}), making them comparable to traditional ALD-precursors in terms of price. Finally, note that other procedures for synthesis of the alkali metal *tert*-butoxides do exist in the literature.¹⁹

III. LiO^tBu IN ALD

The alkali *tert*-butoxide that by far has been utilized the most in ALD is LiO^tBu . This is due to the high interest of lithium containing species in ALD battery research over the last 10 years.²⁰ Although the use of other lithium precursors have been reported [e.g., $Li(thd)$ and $LiN(SiMe_3)$], LiO^tBu is the most commonly used due to exhibiting controllable growth using water as a coreactant.^{21,22} Currently, 27 processes using lithium *tert*-butoxide have been reported and summarized in Table I.

Water has been the predominant oxygen source for lithium *tert*-butoxide, although ozone and oxygen have also been used. The use of these oxygen sources come with certain challenges that must be controlled. O_3 decomposes lithium *tert*-butoxide on the surface, increasing the amount of carbon impurities in the film. The result of $LiO^tBu + O_3$ reaction is most likely lithium carbonate species on the surface, and in some applications, the carbon content may be detrimental to desired functionality. On the other hand, $Li_2O/LiOH$ is hygroscopic, and the use of water is not straightforward either. A significant water reservoir effect may take place, where water is stored in the bulk of the film and is able to react with succeeding precursor pulses in a CVD-like process. This challenge is most predominant in complex compounds, especially if the second metal precursor also reacts with water. This may partly explain the strongly varying GPCs reported as shown in Table I.

In situ analyses of growth mechanisms for otherwise simple processes involving LiO^tBu are not abundant, and for a complete *in situ* study of $Li_2O/LiOH$ ALD chemistry is lacking. It is tempting to attribute this to the difficulty in analysis, not only because of uncertainty of the product, but also because of the lack of self-limitation, possibly due to reservoir effects involving water.^{42,43} A thorough description has, however, been reported for binary Li_2S by Meng *et al.* (Fig. 5).¹⁰ Although there is no reservoir effect taking place here, the principal surface reactions are believed to be comparable to those using water as the coreactant.

Meng *et al.* proposed that the following reactions take place at the surface, initially terminated by $-SH_x$:

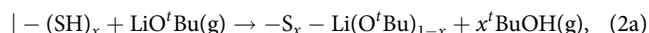


TABLE I. All reported ALD-processes for lithium compounds using lithium *tert*-butoxide as the lithium source. Compiled (11 August, 2020). Me, methyl (–CH₃); Et, ethyl (–CH₂CH₃); ⁱPr, isopropyl (CH₃–CH–CH₃); Cp, cyclopentadienyl; thd, 2,2,6,6-tetramethyl-heptadionato; FMD, formamidinato; pyr, pyridine.

Compound	LiO ^t Bu source T (°C)	Coreactant A	Coreactant B	Coreactant C	T (°C)	GPC (Å/cyc)	Reference
Li ₂ O	160	H ₂ O	—	—	225	N/A	23
LiOH	140	H ₂ O	—	—	50–300	1.2	24
	160	H ₂ O	—	—	225	N/A	21
LiF	160–170	TiF ₄	—	—	250	0.5	25
	135	HF-pyr	—	—	150	0.9	26
	130	NH ₄ F	—	—	150–250	0.5	27
Li ₂ S	140	H ₂ S	—	—	150–300	1.1	10
Li ₂ CO ₃	140	H ₂ O	CO ₂	—	50–300	0.6	24
	140	O ₂ (p)	—	—	50–300	0.82	24
LiAl _x F _y	160–170	AlCl ₃	TiF ₄	—	250	~1	25
LiAl _x O _y	160	H ₂ O	Al(Me) ₃ + O ₃	—	225	~2.8 ^a	28
LiAl _x S _y	140	H ₂ S	Al(NMe ₂) ₃ + H ₂ S	—	150	0.5	29
LiCo _x O _y	120	O ₂ (p)	CoCp ₂ + O ₂ (p)	—	325	~0.6	6
LiNb _x O _y	170	H ₂ O	Nb(OEt) ₅ + H ₂ O	—	35	1.8–2.87 ^b	30
LiP _x O _y	90–110	PO ₄ (Me) ₃	—	—	225–300	0.7–1.0	31
LiSi _x O _y	170	H ₂ O	Si(OEt) ₄ + H ₂ O	—	225–300	0.80–1.36	32
LiTa _x O _y	170	H ₂ O	Ta(OEt) ₅ + H ₂ O	—	225	N/A	33
LiTi _x O _y	130	H ₂ O	Ti(O ⁱ Pr) ₄ + H ₂ O	—	225	1–2 ^c	34
	160	H ₂ O	TiCl ₄ + H ₂ O	—	225	N/A	23
LiAl _x Si _y O _z	160	H ₂ O	Al(Me) ₃ + H ₂ O	Si(OEt) ₄ + H ₂ O	290	20.6 ^d	35
LiFe _x P _y O _z	180	H ₂ O	FeCp ₂ + O ₃	PO ₄ (Me) ₃ + H ₂ O	300	9.4 ^e	36
LiLa _x Ti _y O _z	160	H ₂ O	TiCl ₄ + H ₂ O	La(thd) ₃ + O ₃	225	N/A	21 and 23
LiLa _x Zr _y O _z	N/A	O ₃	La(ⁱ PrFMD) ₃ + O ₃	Zr(NMe ₂) ₄ + O ₃	225	N/A	37
LiP _x O _y N _z	165	H ₂ O	PO ₄ (Me) ₃ + N ₂	—	250	1.05	38
	N/A	PO(NH ₂)(OEt) ₂	—	—	N/A	N/A ^f	39
	100–180	O ₂	P[N(Me) ₂] ₃ + NH ₃	—	350–500	0.72	40
LiTi _x P _y O _z	180	H ₂ O	Ti(O ⁱ Pr) ₄ + H ₂ O	PO ₄ (Me) ₃ + H ₂ O	250	0.87	41

^aSupercycle GPC for 1:1 (Li:Al).

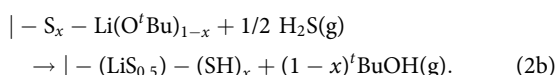
^bSupercycle GPC for varying ratios.

^cSupercycle GPC for varying ratios.

^dSupercycle GPC for 10:6:4, Al:Li:Si.

^eSupercycle GPC for 5:1:1, Fe:Li:P.

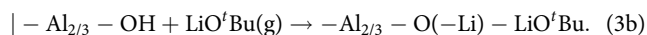
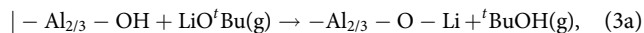
^fArticle claims that LiO^tBu has been tested and gives same results as LiHMDS, but no details are given.



Quartz crystal microbalance (QCM) studies were used to establish that approximately half of the –O^tBu ligands are released during the LiO^tBu pulses, whereas the other half are released during the H₂S pulse for deposition at 150 °C. The fraction released during the two different pulses vary significantly with deposition temperature, with less –O^tBu ligands being released during the LiO^tBu pulses at higher temperatures. This study, however, does not take the oligomeric nature of LiO^tBu into account. Although it does not necessarily change the significance of the released ratios and mass changes that are observed, it does offer an explanation to how –O^tBu ligands can be released upon pulsing of both species. So while it is likely that the oligomeric

lithium *tert*-butoxide partially reacts with the thiol surface giving –S–Li bonds and releasing *tert*-butanol, some of the oligomer is still maintained on the surface and is not released until the succeeding H₂S pulse.

Pertaining to previous reports, the Li₂O/LiOH process using *tert*-butoxide seem to be very compatible with a wide selection of other metal processes. As an example, Aaltonen *et al.* studied the growth of LiAl_xO_y using (LiO^tBu + H₂O) + (TMA + O₃) by QCM (Fig. 6).²⁸ The mass gains observed are explained by two possible reactions upon pulsing LiO^tBu on an aluminum hydroxide terminated surface,



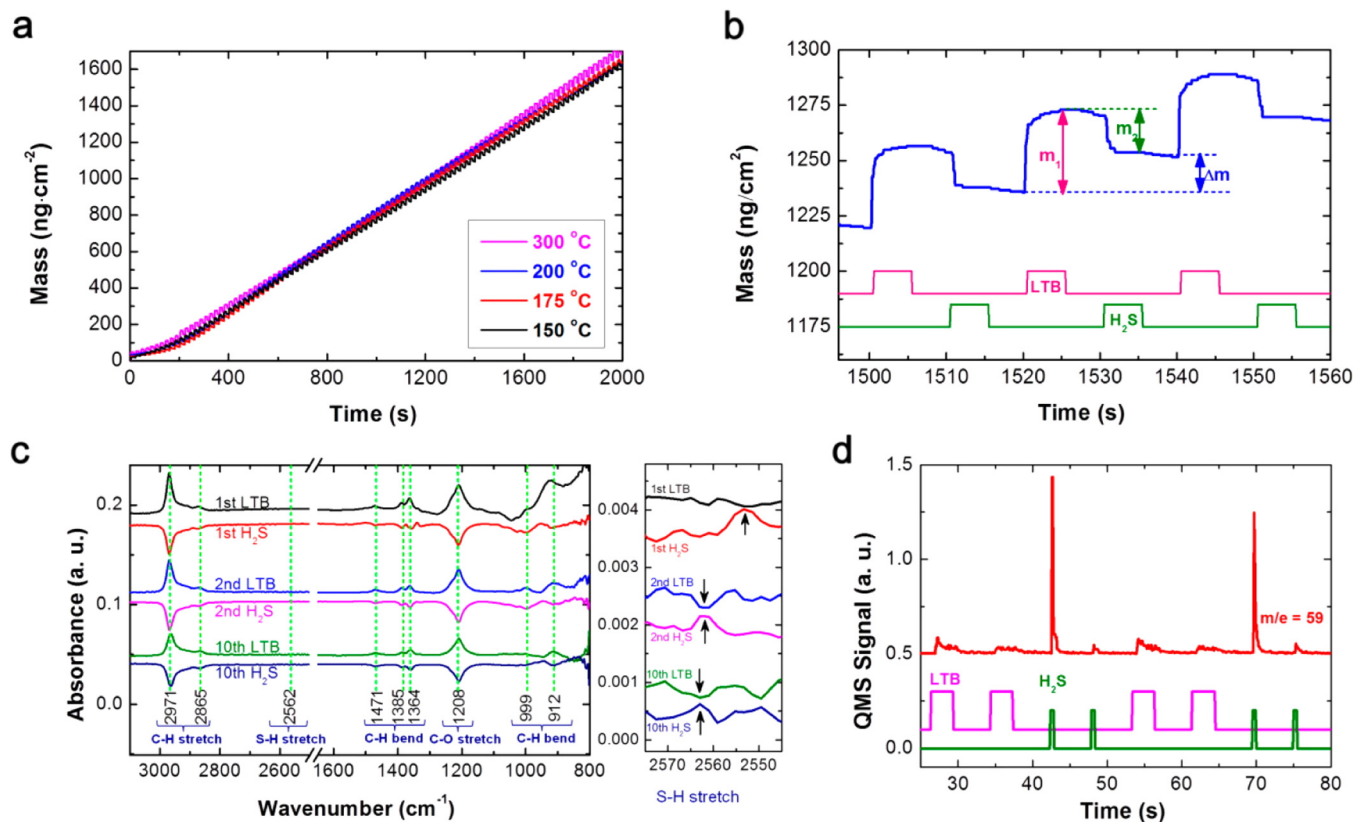
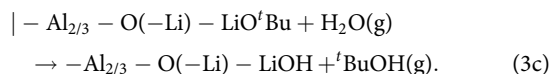


FIG. 5. Investigation of surface chemistry for Li₂S ALD. (a) and (b) *In situ* QCM measurements of Li₂S ALD at 150, 175, 200, and 300 °C using the timing sequence 5–5–5–5 s: (a) mass of Li₂S film vs time during 100 ALD cycles and (b) enlarged view of three consecutive Li₂S ALD cycles performed at 150 °C in the regime of constant growth per cycle (precursor pulsing is indicated by lower traces, and m_1 , m_2 , and Δm are described in the text). (c) *In situ* FTIR difference spectra recorded after individual LTB and H₂S exposures during the first, second, and 10th ALD cycles on an ALD Al₂O₃ surface at 225 °C; right-hand spectra show expanded views of the S–H stretching region. (d) *In situ* quadrupole mass analyzer (QMS) measurements during two consecutive Li₂S ALD cycles at 225 °C, where the LTB and H₂S precursors are each dosed twice (dosing indicated by lower traces) to reveal possible background signals. Reprinted with permission from Meng *et al.*, Chem. Mater. **8**, 10963 (2014). Copyright 2014, American Chemical Society.

For (3b) upon pulsing of water, the *tert*-butoxide group is removed,



Aaltonen *et al.* also raise the question whether the hygroscopic nature of LiOH leads to absorption of crystal water that later works as a reservoir. In any case, this mechanism is in line with what has been reported for Li₂S. It is noteworthy here that equipped with the knowledge that the lithium *tert*-butoxide is an oligomer, reaction (3b) may be a more correct representation of the reactions taking place.

Apart from binary compounds, a range of important complex oxides with lithium have also been deposited, including pyroelectric lithium tantalate, ferroelectric lithium niobate, the important cathode material lithium cobaltite and the electrolyte LiPON.^{6,33,38}

One interesting note from most of these reports is that Li₂O/LiOH seems to grow very fast. Liu *et al.* used extrapolation of GPCs for varying LiO^{*t*}Bu to Ta(OEt)₅ pulsed ratios to estimate a GPC of ~1.7 Å/cyc for Li₂O (Fig. 7).³³ This would require the deposition of 1/2 of a monolayer per cycle, which is higher than what is traditionally acceptable given the size and the attainable adsorbed surface areal density of the precursor. The oligomeric conformer of LiO^{*t*}Bu can again help explain this, as it has a very high density of Li-atoms if adsorbed as an oligomer. Furthermore, the Liu *et al.* study showed that a 1:1 pulsed ratio between LiO^{*t*}Bu and Ta(OEt)₅ results in a 12:1 cation ratio in the films. Even if Ta₂O₅ has a significantly lower growth rate than Li₂O/LiOH, this ratio far exceeds what can be expected. It is possible that LiOH (and eventually Li₂CO₃) is incorporated in the film either via diffusion into the film or via reaction with the *tert*-butoxide oligomer.

In other words, one has to be careful when employing LiO^{*t*}Bu in ALD of complex compounds and be prepared to fine-tune the

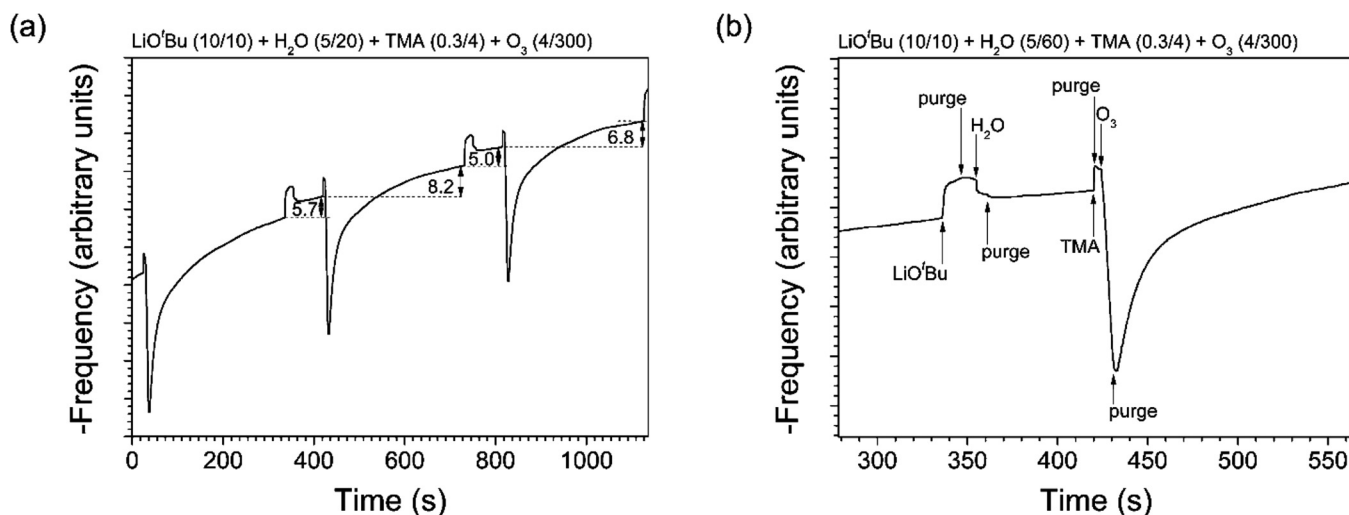


FIG. 6. (a) QCM data collected during the (LiO'Bu + H₂O) + (TMA + O₃) pulsing sequence at 225 °C, where (b) the onset of the pulse and purge periods are indicated by arrows. Reprinted with permission from Aaltonen *et al.*, Chem. Mater. **23**, 4669 (2011). Copyright 2011, American Chemical Society.

pulsed ratios between the cation precursors. As the hygroscopic nature of LiOH makes the process sensitive to water dosing and possibly water partial pressure over the substrate, further attention is required during process development. The biggest advantage of the LiO'Bu + H₂O process is a relatively clean chemistry, minimizing unwanted carbonate in the resulting films.

Some care should be taken with respect to ligand types for coreactants in these processes. As an example, Aaltonen *et al.* observed a significant amount of chlorine in lithium tantalate films

deposited using LiO'Bu and TiCl₄.²³ Due to the very high surface loading of lithium during a cycle, it is important to avoid ligands that form very stable compounds with lithium. In Aaltonen *et al.*'s case, lithium chloride is very likely to have formed.

A final note should be made on the varying source temperatures used for LiO'Bu. Reports vary between 100 and 180 °C, with the majority of studies carried out between 140 and 170 °C. Suitable source temperatures vary depending on reactor type, chamber pressure, and geometry, with lower temperatures reported

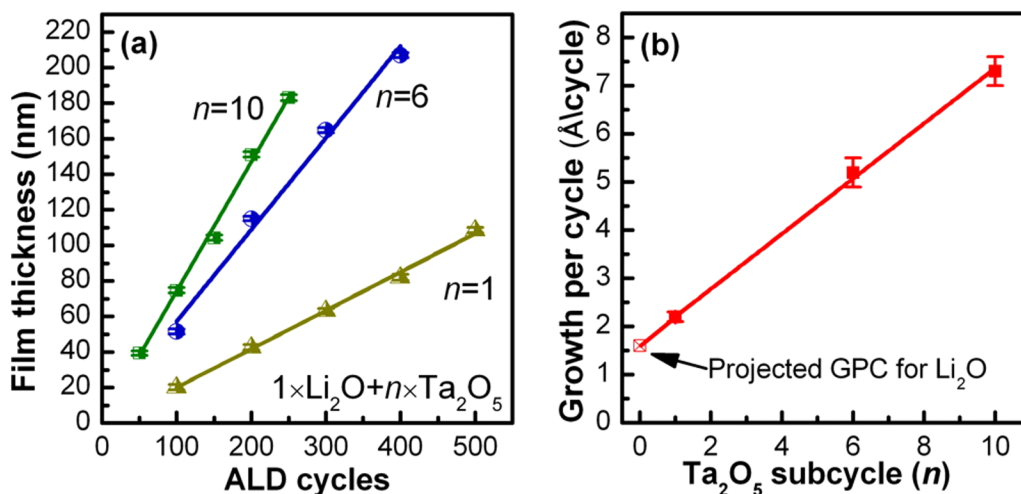


FIG. 7. (a) Thickness of the lithium tantalate thin films as a function of ALD cycle number and (b) the growth per cycle of the lithium tantalate thin films as a function of Ta₂O₅ subcycle number, using pulsing sequences of 1 × Li₂O + n × Ta₂O₅ (n = 1, 6, and 10). Reprinted with permission from Liu *et al.*, J. Phys. Chem. C **117**, 20260 (2013). Copyright 2013, American Chemical Society.

for depositions using an inert gas valving where the precursor resides inside the reactor itself. These reported source temperatures may also be affected by inadvertent exposure of the LiO^tBu to humidity to create an encapsulating hydroxide skin as discussed above. Since reports on saturated surface chemistry using the LiO^tBu are somewhat limited, it becomes difficult to consider a particular source temperature as the most suitable one for ALD process. Thus, the reader should take note that the reported values in Table I are best not to be directly employed but must be tailored to the particular reactor tool and process conditions.

IV. NaO^tBu IN ALD

Interest in sodium containing species is expected to increase with the introduction of sodium ion batteries as low-cost alternatives to their lithium counterparts. Reports on ALD of sodium containing films are sparse, with NaAl_xO_y , NaNb_xO_y , NaTi_xO_y , NaTa_xO_y , and NaCoO_2 being the only compounds found in the literature.^{8,9,13,44,45} All these processes have made use of NaO^tBu , except for NaCoO_2 where the β -diketonate $\text{Na}(\text{thd})$ was successfully employed. Sodium ALD suffers from the same challenge as lithium, being very difficult to characterize due to the instability of $\text{Na}_2\text{O}/\text{NaOH}$ upon contact with air.

The inaugural work on sodium ALD is quite recent, being published as late as in 2014 by Østreg *et al.*, where several different Na-precursors were evaluated and the *tert*-butoxide was found to offer the cleanest chemistry.¹³ NaO^tBu was studied by combining $\text{NaO}^t\text{Bu} + \text{H}_2\text{O}/\text{O}_3$ with the well-known TMA + $\text{H}_2\text{O}/\text{O}_3$ process to deposit NaAl_xO_y . The evaluation points toward a very

similar chemistry as found for lithium, with high growth rates and rapid incorporation of Na even for low pulsed ratios (Fig. 8).

One major difference is observed for sodium containing multi-cation processes from its lithium counterpart, especially when water is used as the oxygen source. When the incorporated amount of Na tends toward a limit value (50% in the case of NaAl_xO_y), additional cycles of $\text{NaO}^t\text{Bu} + \text{H}_2\text{O}$ do not increase the alkali metal content significantly. Effectively, this means that two subsequent subcycles of $\text{NaO}^t\text{Bu} + \text{H}_2\text{O}$ does not deposit higher Na content than one sub-cycle. This could mean that an $[-\text{NaOH}]$ terminated surface does not facilitate continued growth of $\text{Na}_2\text{O}/\text{NaOH}$. Note that this effect is not present when O_3 is used as the oxygen source, indicating that $[-\text{NaOH}]$ termination affects continued growth differently as compared to $[-\text{Na-O}^*]$. The same study used *ex situ* FT-IR measurements to look for evidence of carbonates which could hamper successive growth. Quite surprisingly, it was found that the films where O_3 is used show less incorporation of carbonate as compared to the water based process (Fig. 9). This indicates that the *tert*-butoxide ligands do not decompose into carbonates upon O_3 exposure, but rather form volatile carbon species that are purged out of the reaction chamber. The carbonate incorporated by the water process is most likely attributed to postdeposition reactions when exposed to air. Although water based chemistry is often appreciated due to its simplicity, it should be noted that O_3 may be the preferred oxygen source for ALD using the alkali *tert*-butoxides.

The use of sodium *tert*-butoxide for deposition of NaNbO_3 and NaTaO_3 using a water based process confirms the observed behavior previously reported by Østreg *et al.*⁸ Sodium is incorporated very fast, reaching 50 cat. % Na at a pulsed ratio of 1:3 (Fig. 10). After

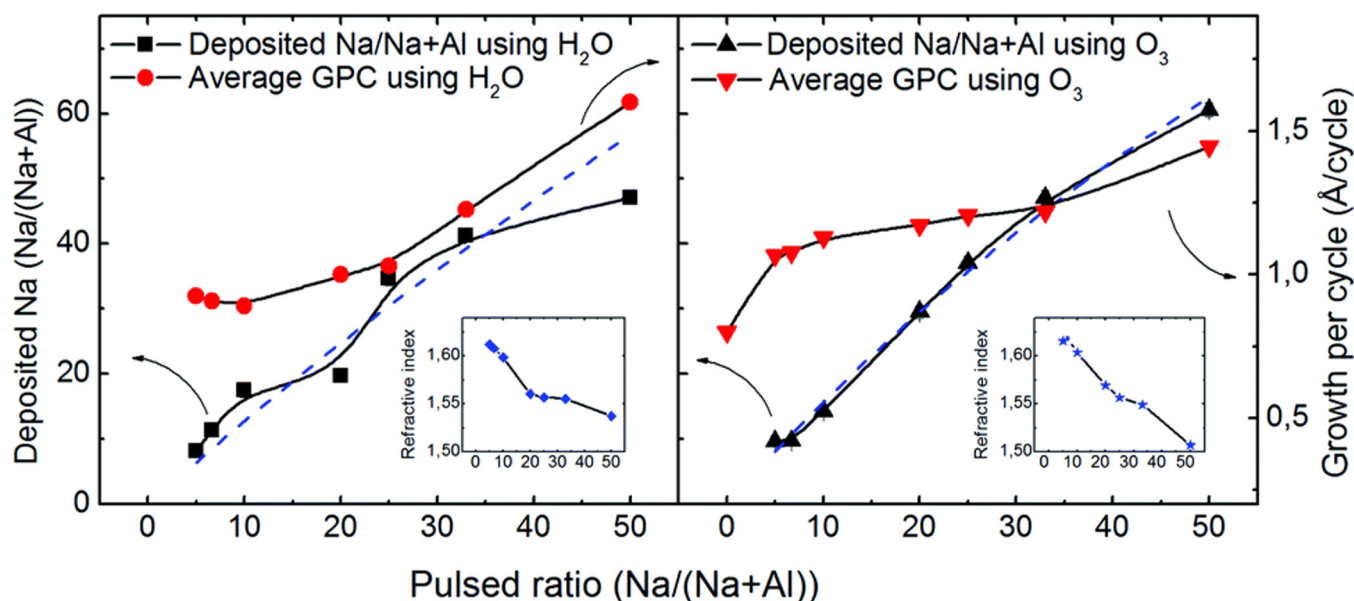


FIG. 8. Refractive index, growth rate, and deposited composition using 500 total cycles on silicon at 250 °C with varying ratios of NaO^tBu and TMA with either H_2O or O_3 as oxygen source. NaO^tBu was kept at 140 °C and 0.5 s pulses were used. The blue dashed line is the best fit of the surface utilization model. Reprinted with permission from Østreg *et al.*, Dalton Trans. 43, 16666 (2014). Copyright 2014, Royal Society of Chemistry.

reaching 50 cat. %, the incorporation significantly slows down. Films with high amounts of Na (>50 cat. %) are also reported to rapidly become opaque when exposed to air. This point toward the formation of NaOH or Na₂CO₃. The ALD temperature-window for the Na(Nb,Ta)O₃ processes were also studied in the same report. GPCs are constant within uncertainties between 200 and 300 °C, before rapidly decreasing at higher temperatures (Fig. 11). The reduced GPC at higher temperatures is in line with, e.g., Hornsveld *et al.* for the deposition of Li₂CO₃.²⁴

One of the most attractive features of ALD is its ability to deposit thin films on high aspect ratio substrates, due to the self-limiting surface reactions that take place, ruling out the need for line-of-sight. Depending on the process and precursors used, however, deposition on topologically complex substrates is not always straightforward. Liu *et al.* reported growth of NaTi_xO_y on carbon nanotubes and anodic aluminum oxide templates, and found that the incorporation of Na was uniform even on these topologies (Fig. 12).³³ This significantly increases the impact of sodium *tert*-butoxide as an ALD precursor for future 3D battery materials, for which other deposition techniques fall short.

The ALD of sodium-containing films is still in its infancy, and many interesting materials are yet to be reported. This includes, i.e., sodium vanadate which is believed to be possible candidates as sodium battery cathodes. Sodium *tert*-butoxide as an ALD precursor opens up for a wide range of possibilities that were not attainable only a few years ago.

V. Ko^tBu IN ALD

Interest in potassium ALD has been limited by the apparent lack of technologically interesting compounds containing potassium.

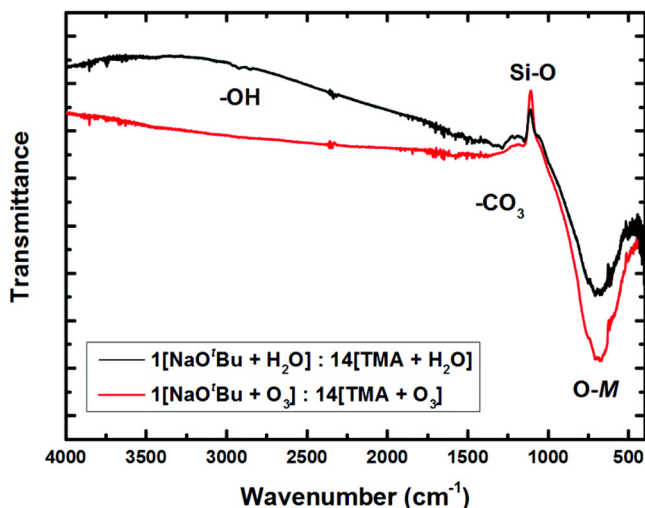


FIG. 9. Representative FTIR-spectra of samples deposited using a 1:14 ratio of sodium to aluminum using water or O₃ as an oxygen precursor. The black (top) and red (bottom) line show films deposited with water and O₃, respectively. Reprinted with permission from Østreg *et al.*, Dalton Trans. **43**, 16666 (2014). Copyright 2014, Royal Society of Chemistry.

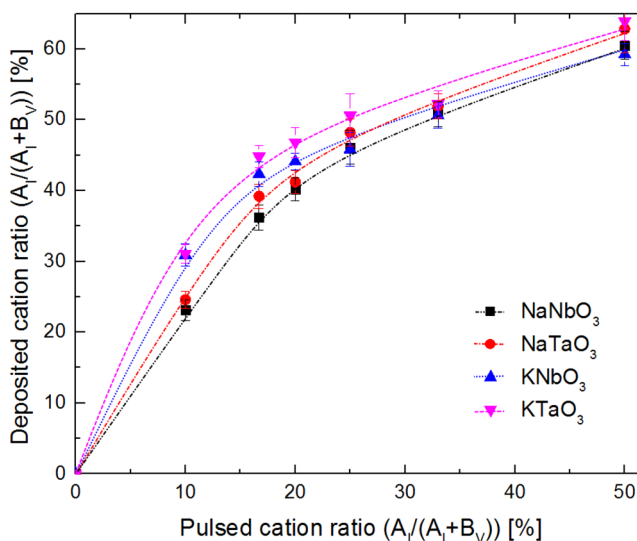


FIG. 10. Growth rate of the A'B'V₃O₃-systems as a function of pulsed cationic ratio. Reprinted with permission from Sønsteby *et al.*, J. Vac. Sci. Technol. A **34**, 041508 (2016). Copyright 2016, American Vacuum Society.

Although potassium batteries have been discussed, they have always been outcompeted by lighter lithium- and sodium variants, offering very little additional cell potential or stability. Outside battery research, however, there are some highly appreciable compounds

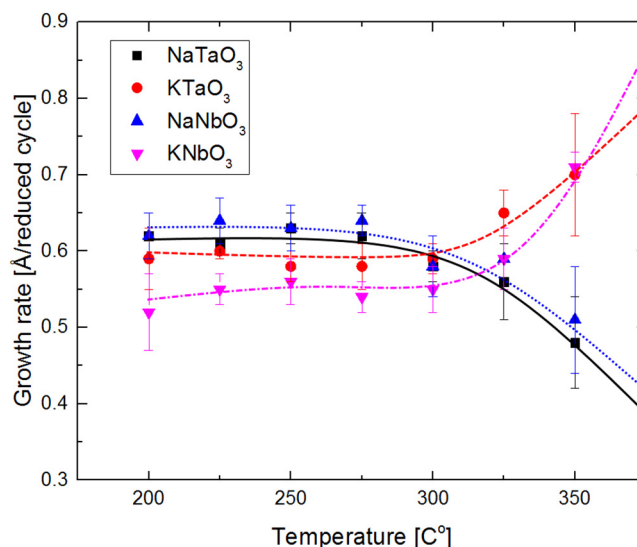


FIG. 11. GPC for the NaNbO₃, NaTaO₃, KNbO₃, and KTaO₃ thin films as a function of reactor temperature. All films were deposited using a 1:3 alkali vs group V metal pulsing ratio. Reprinted with permission from Sønsteby *et al.*, J. Vac. Sci. Technol. A **34**, 041508 (2016). Copyright 2016, American Vacuum Society.

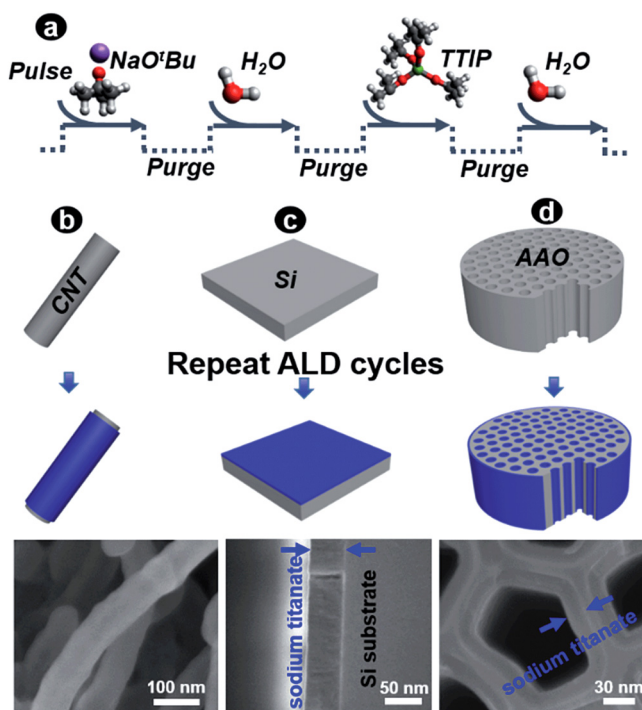


FIG. 12. (a) One ALD cycle of sodium titanates consists of a sequential pulse of NaO'Bu, H₂O, TTIP, and H₂O, with an N₂ gas purge after each pulse. By repeating the above sequence in a cyclic manner, uniform, conformal sodium titanate films (blue color) are deposited on (b) nitrogen-doped CNTs, (c) Si wafer, and (d) AAO template (surface polished with sandpapers). Reprinted with permission from Liu *et al.*, *J. Phys. Chem. C* **117**, 20260 (2013). Copyright 2013, American Chemical Society.

where potassium is a major component. This includes the important electro optical material K(Nb,Ta)O₃, and ferroelectric KNbO₃.^{46,47} The mixed A-site ferroelectric (K,Na)NbO₃ is also proposed to be a contender to abolish the PZT hegemony of ferroelectrics, as it provides similar piezoelectric constants without the need for toxic lead.³

Potassium ALD was introduced in the same inaugural work as sodium.¹³ *tert*-butoxide was again found to be the only viable option out of the precursors tested, offering clean one-step sublimation. Deposition was carried out using KO'Bu + H₂O together with TMA + H₂O and showed a similar trend in K-incorporation as compared to Na (Fig. 13). One interesting feature in this process is that the limit for K-incorporation seems to be as low as 30 cat. % in the alumina matrix.

Østreg *et al.* also studied the temperature dependence of the growth of KAlO_x (Fig. 14) and found a similar effect to what was observed for the deposition of KNbO₃ and KTaO₃ (Fig. 11).⁸ At increased temperatures, the GPC significantly increases, possibly due to the decomposition of the precursor. High carbon contents have been observed by x-ray photoelectron spectroscopy (XPS) for films deposited above 300 °C. This differs from the NaO'Bu and

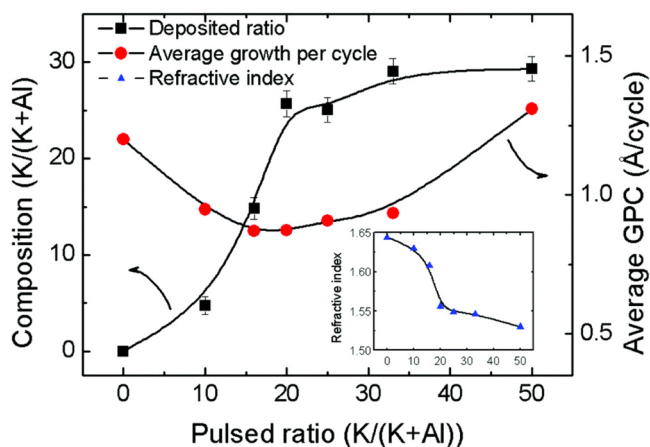


FIG. 13. Refractive index and deposited composition using 500 total cycles on silicon at 250 °C with varying ratios of KO'Bu and TMA with H₂O an oxygen source. The KO'Bu was kept at 170 °C and using 1 s pulses. Reprinted with permission from Østreg *et al.*, *Dalton Trans.* **43**, 16666 (2014). Copyright 2014, Royal Society of Chemistry.

LiO'Bu temperature dependency, where the GPC was shown to be significantly *reduced* upon increased temperature. Note here that the structure of KO'Bu also differs from the Na- and Li-variants, as it adopts as a cubanelike tetramer. Furthermore, the more electro-positive potassium exhibits higher ionicity, possibly creating a stronger bond toward the surface, such that decomposition of the precursor takes place before desorption.

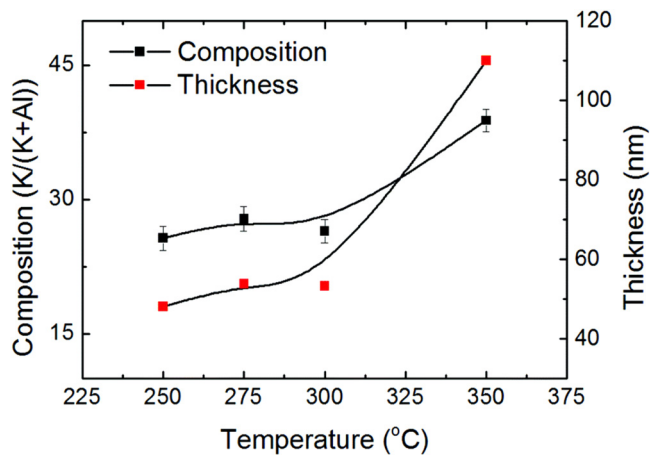


FIG. 14. Growth per cycle and composition of samples deposited using 100 supercycles consisting of 1 cycle KO'Bu and water and 4 cycles of TMA and water deposited at various temperatures. KO'Bu was kept at 170 °C and pulsed for 1 s. Thickness for the sample deposited at 350 °C was estimated from XRF-measurements. Reprinted with permission from Østreg *et al.*, *Dalton Trans.* **43**, 16666 (2014). Copyright 2014, Royal Society of Chemistry.

Another general feature of the alkali metal *tert*-butoxide processes is the manifestation of a *memory effect*. Preceding depositions containing alkali metals appears to affect the cation content in the subsequent films. This effect has been thoroughly studied for potassium *tert*-butoxide during growth of KNbO_3 , as shown by Killi (Fig. 15), by studying K-incorporation in Nb_2O_5 thin films deposited directly after KNbO_3 with varying K-concentration. A significant amount of K is incorporated, with a clear trend in increased amounts for higher K-concentration in preceding depositions. The reason for this is not fully understood, but it is speculated that the reactor itself becomes contaminated with species on the reactor walls that become volatile during the succeeding deposition. The effect can be worked around by either passivating the reactor by depositing an inert oxide (e.g., Nb_2O_5 or Al_2O_3) or by cleaning the reactor between depositions. The former has been used in the deposition of $(\text{K,Na})\text{NbO}_3$, exhibiting high reproducibility.⁹

Sønsteby *et al.* recently studied the mechanistic behavior of KO^tBu by means of QCM and FT-IR.¹¹ Clear evidence was reported that the high GPC is a result of two major contributions. The first is a dense chemisorption of tetramer KO^tBu , which reacts with water from the succeeding water pulse to form large amounts of KOH . This creates an effect very similar to what was observed for Li in the deposition of LiTaO_3 .³³ The other is a *reservoir effect*, where the hygroscopic nature of the film bulk and KOH surface species absorb water that later reacts with subsequent pulses. In the same study, ternary KNbO_3 was also studied in depth (Fig. 16), showing that the deposited ratio of KOH with respect to the other cation precursor alters the growth significantly. High concentrations of KOH slows down growth of the other cation precursor. Furthermore, Sønsteby *et al.* also found that the observed mass

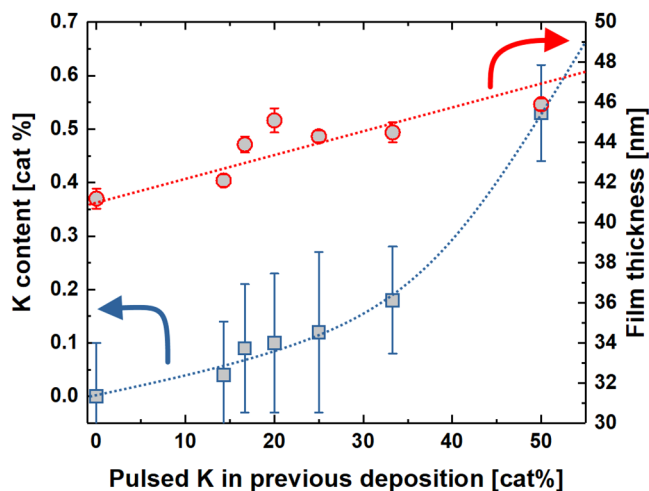


FIG. 15. Potassium content in Nb_2O_5 films deposited at 250°C from niobium ethoxide and water, as a function of the amount of pulsed potassium in the preceding deposition. The blue curve (left axis) shows the potassium content (cat. %), while the red curve (right axis) shows the film thickness. Reproduced with permission from V. A.-L. K. Killi, "The role of passivation in deposition of thin films of K_xNbO_3 ," B.Sc. thesis, University of Oslo (2018) (Ref. 54).

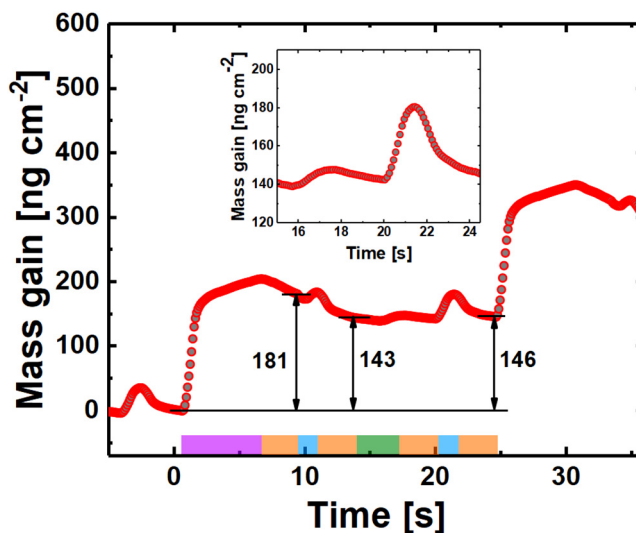


FIG. 16. One representative supercycle of 1:1 pulsing $[\text{Nb}(\text{OEt})_5 + \text{H}_2\text{O} : \text{KO}^t\text{Bu} + \text{H}_2\text{O}]$ as measured by QCM. Colored fields indicate (from left to right) KO^tBu pulse (purple), purge (orange), water pulse (blue), and $\text{Nb}(\text{OEt})_5$ pulse (green), respectively. The inset shows a zoomed in version of the response for $\text{Nb}(\text{OEt})_5 + \text{H}_2\text{O}$. Sønsteby *et al.*, Dalton Trans. 49, 13233 (2020). Copyright 2020, Royal Society of Chemistry.

gains as measured by QCM do not conform to the deposited cation ratios in the films.¹² A substitution reaction with KOH reacting with ligands from $\text{Nb}(\text{OEt})_5$ to form volatile KOEt was proposed to explain this observation.

The lesson learned is that the structure and ionicity of KO^tBu lead to quite different behavior compared to its Li- and Na counterparts. KOH that is formed during deposition is highly hygroscopic and forms a water reservoir that alters growth of succeeding cycles. A high deposited K-content (>50 cat. %) leads to uncontrolled growth that becomes very dependent on the water dose, and the films produced readily react with air after breaking vacuum. In other words, using KO^tBu as an ALD precursor is not straightforward, but these complicating factors can be controlled by careful process control and understanding of the underlying mechanisms. Furthermore, the recent success of depositing sodium containing films using $\text{Na}(\text{thd})$ suggests that $\text{K}(\text{thd})$ might be possible to employ for potassium ALD as an alternative to KO^tBu .

VI. RbO^tBu IN ALD

Rubidium *tert*-butoxide was first introduced as an ALD-precursor in 2017.¹⁷ It adopts a structure similar to potassium *tert*-butoxide with a tetrameric oligomer, and it is believed to behave very similar in terms of surface reactions. Currently, only one report on its use is found in the literature, containing information on the deposition of $\text{Rb}:\text{TiO}_2$ and RbNbO_3 . However, interest in the deposition of rubidium containing compounds is expected to increase with its newfound application in perovskite solar cells. This has become even more relevant after the successful ALD of

PbI₂, opening for more ALD studies on tandem perovskite solar cells.⁴⁸ In addition, (K,Rb)NbO₃ and variants thereof is theoretically shown to be a tunable ferroelectric much like KNN, but obtaining the functional perovskite phase has proven very difficult with most synthesis techniques.⁴⁹

RbO^tBu is found to offer self-limiting behavior in combination with a second cation precursor for the deposition of a ternary compound (Fig. 17). High stoichiometric control is attainable with ALD, shown by the possibility of Rb acting as a minor dopant in a TiO₂-matrix, and as a major component in RbNbO₃ perovskite.

One interesting deviation from all the lighter alkali metal processes is a very distinct relationship in the pulsed to deposited cation ratios (Fig. 18). This was studied for the RbNbO₃-process and should in other words be comparable to growth of NaNbO₃ and KNbO₃.

The cation content increases rapidly up to approximately 20 cat. % before reaching a plateau. Above 15% pulsed RbO^tBu, the incorporation again rapidly increases, and at 20% pulsed RbO^tBu, there is 50 cat. % Rb in the films. This is accompanied by larger gradients and more uncontrolled growth, with films visibly reacting with air upon breaking vacuum. At 25% pulsed RbO^tBu the gradient is more than 10%, and there seems to be no limitation in the amount of Rb that can be incorporated.

One should note here, however, that pulsed ratios above 25% have not been studied, in other words there are always Nb (OEt)₅-pulses preceding pulses of RbO^tBu. For KO^tBu and NaO^tBu, incorporation of the alkali element slowed down for pulsed ratios above 50% (i.e., for succeeding subcycles of, e.g., KO^tBu + H₂O), and it is possible that a similar effect exists also for

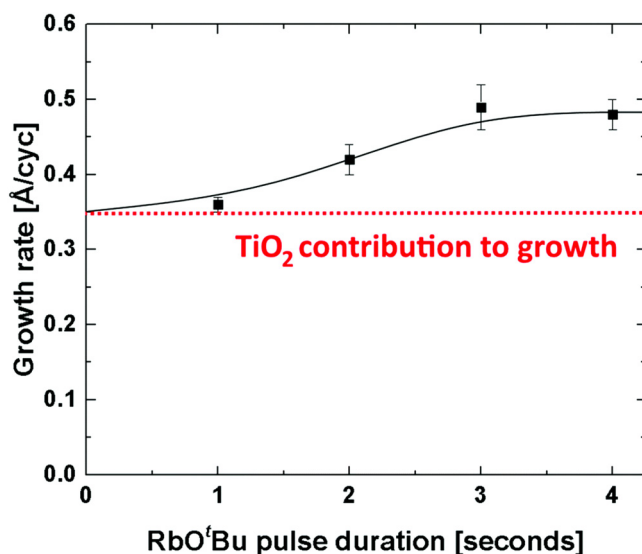


FIG. 17. Growth rate as a function of RbO^tBu pulse duration. Depositions were carried out at a 1 : 11 RbO^tBu : TTIP ratio with 5 s TTIP, water, and purge durations. The dashed red line shows the theoretical minimum growth rate for a "virtual" 0 s pulse, corresponding to TiO₂ growth. Sønsteby *et al.*, Dalton Trans. **46**, 16139 (2017). Copyright 2017, Royal Society of Chemistry.

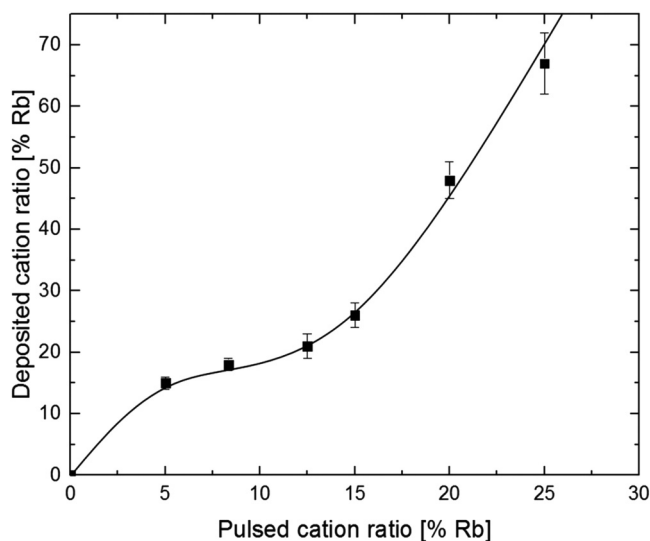


FIG. 18. Deposited cation ratio as a function of % RbO^tBu pulses in the Rb-Nb-O system, measured by x-ray fluorescence. Uncertainties in the data are given by the Stratos model used to fit the collected fluorescence spectra. Sønsteby *et al.*, Dalton Trans. **46**, 16139 (2017). Copyright 2017, Royal Society of Chemistry.

RbO^tBu. In any case, this would be at a very high level of incorporated Rb, where the films would not be stable toward air. It is also likely that RbO^tBu forms Rb₂O/RbOH on the surface during film growth, leading to the same issues that were found for lithium and potassium (i.e., memory and reservoir effects). Nonetheless, additional studies are needed to fully understand the reactions taking place during growth using RbO^tBu, as there are some obvious differences with respect to the lighter alkali *tert*-butoxides.

VII. CsO^tBu IN ALD

We arrive at the heaviest of the non-radioactive alkali metals, and the only one that has not previously been reported in the ALD-literature. CsO^tBu is known to adopt a similar oligomer compared to KO^tBu and RbO^tBu, with tetramer units that readily react with water. The ionicity and hygroscopicity is even stronger for the Cs-variant, but for practical purposes, the reaction mechanisms and pitfalls are thought to be similar. In other words, it is only natural to think that cesium *tert*-butoxide could enable ALD-growth of cesium-containing compounds.

Cs-containing materials are currently observing a massive boost in interest, due to the use of β -CsPbI₃ in high efficiency perovskite tandem solar cells.⁵⁰ With the previously mentioned success in ALD of PbI₂, CsPbI₃ can definitely be the next step.⁴⁸ The only limitation has been the lack of reported processes for Cs.

For the sake of a comparative evaluation of the alkali metal *tert*-butoxides as ALD precursors, we have carried out some initial studies of Cs-containing deposition by employing CsO^tBu (experimental information in the supplementary material⁵³). Current results show the same trends as KO^tBu and RbO^tBu, with extremely

rapid incorporation of Cs and high GPCs, even for low amounts of pulsed CsO^tBu. The issue we have faced is the lack of complex oxides that stabilize CsO_x/CsOH, resulting in films that rapidly react with air upon breaking vacuum.

We have, however, been successful in incorporating Cs in thin films via ALD in an NbO_x matrix, as measured by XPS (Fig. 19). The films visually react upon extraction from the reactor, probably with H₂O or CO₂ in air, forming what looks like a liquid surface. This is likely due to the hygroscopic nature of Cs₂O/CsOH/Cs₂CO₃, similar to what is observed for the other alkali metal systems. The presence of carbon as carbonate is confirmed by the XPS spectra (see detailed XPS scans in the supplementary material⁵³). Eventually, the liquid seems to dry out, and the result is a relatively uniform film, especially for low pulsed ratios of CsO^tBu. Pulsed ratios higher than 5:1 [Nb(OEt)₅:CsO^tBu] result in more than 50 cat. % Cs in the film. In other words, the same behavior as the lighter alkali versions but even more extreme. The higher pulsed ratios do not increase the amount of Cs in the films dramatically (it remains slightly above 50%), but the uniformity of the films become dramatically worse with more pulses of CsO^tBu, possibly due to additional formation of Cs₂CO₃.

More work is needed to recognize CsO^tBu as a viable precursor for Cs-incorporation in ALD. It is clear that the precursor itself is volatile and chemisorbs to the surface, and that it reacts with water. Given the extreme growth observed, however, it is possible that other Cs-precursors that do not react as violently or that can be used without water as a coreactant are better choices.

Still, we believe that the CsO^tBu + H₂O process can be controlled, but that a more stabilizing chemical environment is required for a proper investigation. This could, e.g., be Cs-deposition together with PbI₂, which could lead to an ALD-breakthrough in the synthesis of perovskite tandem solar cell materials. The CsPbI₃ perovskite structure is much more stable and less reactive than, e.g., CsNbO₃, and would make for a better platform for studying cesium growth. Another possibility is employing CsO^tBu together with O₃, to avoid water storage and effects stemming from the hygroscopicity. This may come at the cost of increased carbon contamination as observed for lithium, but this remains to be seen. In any case, by enabling a route for Cs-incorporation, we eagerly await reports from the community on combining this process with PbI₂.

VIII. A NOTE ON COMBINING ALKALI *tert*-BUTOXIDES

As a final note, we discuss the possibility of combining alkali metal *tert*-butoxides to enable growth of quarternary compounds. This opens for functional materials with mixed alkali-metal sites that can be used to tune functional properties. One example in this respect is K_xNa_{1-x}NbO₃, which exhibits several morphotropic phase boundaries where its piezoelectric response is enhanced.⁵¹ Studies on other quarternary systems show that limiting the amount of precursor types is beneficial to obtain control of the deposited composition. This is very likely an effect of that similar precursor types lead to similar chemistries allowing for direct substitution of precursor half-cycles in a host binary process. This is seen, e.g., in the deposition of Sr:LaFeO₃, where use of La(thd)₃, Sr(thd)₂, and Fe(thd)₃ makes the system behave *pseudobinary*, and tuning the stoichiometry is a straightforward cation precursor substitution.⁵² In other words: It is convenient to have precursors with similar chemistries when trying to make quarternary/quinary compounds, as the systems then often behave *pseudobinary* or *pseudoternary*.

Although there are differences in the growth behavior of the alkali *tert*-butoxide going from NaO^tBu to KO^tBu, many of the same reaction types are taking place on the surface, with similar qualitative results. Thus, quarternary compounds can be, and have been, deposited with success. Sønsteby *et al.* carried out a study on KNN, where the recipe for KNbO₃ was used as basis.^{8,9} KO^tBu was then gradually substituted with NaO^tBu in an attempt to cover the whole KNbO₃-NaNbO₃ composition range. It was found that the K:Na ratio could be tuned at a 1 cat. % level, with high reproducibility and control (Fig. 20). This was later used to deposit KNN thin films with appreciable piezoelectric functionality, a compound that has been intrinsically difficult to deposit with other technique due to the volatility of the alkali oxides at elevated temperatures.

It is important to note here, that this *pseudobinary* process is only applicable at temperatures below 300 °C, since the behavior of the two precursors is radically different above this temperature (Fig. 12). NaO^tBu seems to desorb leading to reduced GPC, while the more ionic KO^tBu seems to decompose on the surface, leading to accelerating GPC. This is manifested as a large deviation in pulsed-to-deposited composition ratios, making direct substitution inapplicable. A similar result has been seen in the deposition of

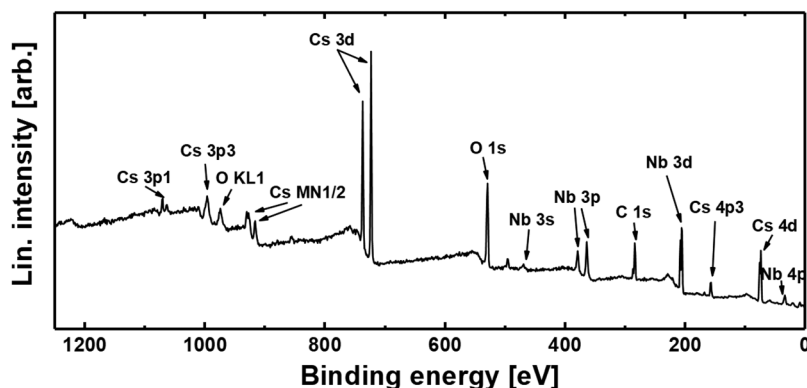


FIG. 19. Representative XPS survey spectra of a Cs-Nb-O film deposited at a 1:5 [CsO^tBu/Nb(OEt)₅] ratio, giving a Cs:Nb ratio of close to 1:1.

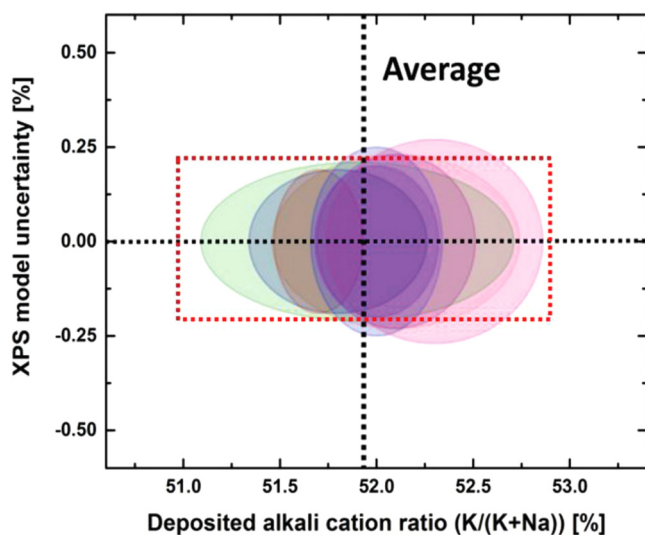


FIG. 20. Eight consecutive depositions using exactly the same parameters (with Nb_2O_5 passivation in between every deposition). Ellipses show the variation in deposited alkali ratio $[\text{K}/(\text{K}+\text{Na})]$, maximum across all directions in the chamber, x axis], and the uncertainty in the XPS-model, y-direction. The dimensions of the red box illustrate the expected variation in deposited stoichiometry by adding one additional pulse of one of the alkaline elements, x-direction, and the instrumental uncertainty of the XPS system, y-direction. Reproduced with permission from *Sønsteby et al.*, *Glob. Chall.* **3**, 180014 (2019). Copyright 2019, Wiley.

quarternary $(\text{Na},\text{K})\text{TaO}_3$ and $(\text{Na},\text{K})(\text{Nb},\text{Ta})\text{O}_3$, all behaving as *pseudoternary* systems with smooth compositional tunability.

We believe that the possibility of using the same precursor type for all the alkali metals can facilitate a range of interesting studies on mixed alkali metal containing compounds, with a novel functionality.

IX. SUMMARY AND CONCLUSIONS

In this paper, we have summarized the existing ALD literature on alkali metal *tert*-butoxides, showing how these precursors enable the deposition of important functional compounds for a more sustainable future. We have shown that *tert*-butoxides are applicable precursors for ALD of all the nonradioactive alkali metals (Li, Na, K, Rb, and Cs). The *tert*-butoxides do not react as monomers, but instead adopt an oligomeric form that is maintained until subsequent coreactant pulses. The structure and ionicity of the precursors are important, shown by the similarity of LiO^tBu and NaO^tBu (which are hexamers), and KO^tBu , RbO^tBu and CsO^tBu (which are tetramers). They all readily react with moisture in air, thus care should be taken when handling the precursor, e.g., for precursor loading. All of the precursors seem to deposit large amounts of hydroxides upon subsequent pulsing of water, leading to an increasing water reservoir during growth. This strongly affects succeeding pulses of other cation precursors in ternary and quarternary processes. Note that the hygroscopicity seems to increase toward the heavier alkali metals, making, e.g., cesium containing deposition

quite difficult to control. Nonetheless, we have shown successful incorporation of Cs by ALD for the first time. The inherent moisture sensitivity of the *tert*-butoxides is a drawback, but one that can be controlled. We do believe, however, that atomic layer deposition of group 1 element compounds would benefit from development of novel precursors that can reduce the moisture sensitivity and thus reduce the observed reservoir effects. Alternatives do exist for Li and Na [$\text{Li}(\text{thd})$, $\text{LiN}(\text{SiMe}_3)_2$, LiOSiMe_3 , and $\text{Na}(\text{thd})$ have been reported], but we believe that there is room for a deeper investigation of possible group 1 precursors. Using the *tert*-butoxides with other oxygen sources (such as O_3) to remove water reservoir effects should also be explored. Finally, we have shown how the careful use of process parameters can enable the use of two *tert*-butoxides in the same process, allowing for the deposition of quarternary materials in a *pseudoternary* process. The possibility of depositing a range of both ternary and mixed alkali quarternary compounds opens up for depositing important sustainable functional materials.

ACKNOWLEDGMENTS

This work was partially carried out within the RIDSEM-project, financed in full by the Research Council of Norway (Project No. 272253). Jeffrey W. Elam was supported as part of the Advanced Materials for Energy-Water Systems (AMEWS) Center, an Energy Frontier Research Center funded by the U.S. Department of Energy (DOE), Office of Science, Basic Energy Sciences, under Contract No. DE-AC02-06CH11357.

REFERENCES

- 1 J. Watts, *Lancet* **374**, 868 (2009).
- 2 M. A. Skundin, T. L. Kulova, and A. B. Yaroslavl'tsev, *Russ. J. Electrochem.* **54**, 113 (2018).
- 3 C.-H. Hong, H.-P. Kim, B.-Y. Choi, H.-S. Han, J. S. Son, C. W. Ahn, and W. Jo, *J. Materiomics* **2**, 1 (2016).
- 4 T. Duong *et al.*, *Adv. Energy Mater.* **7**, 1700228 (2017).
- 5 M. Zhang *et al.*, *ACS Energy Lett.* **2**, 438 (2017).
- 6 M. E. Donders, W. M. Arnoldbik, H. C. M. Knoops, W. M. M. Kessels, and P. H. L. Notten, *J. Electrochem. Soc.* **160**, A3066 (2013).
- 7 J. R. Bickford, H. H. Sønsteby, N. A. Strnad, P. Y. Zavalij, and R. C. Hoffman, *J. Vac. Sci. Technol. A* **37**, 020904 (2019).
- 8 H. H. Sønsteby, O. Nilsen, and H. Fjellvåg, *J. Vac. Sci. Technol. A* **34**, 041508 (2016).
- 9 H. H. Sønsteby, O. Nilsen, and H. Fjellvåg, *Glob. Chall.* **3**, 1800114 (2019).
- 10 X. Meng, D. J. Comstock, T. T. Fister, and J. W. Elam, *ACS Nano* **8**, 10963 (2014).
- 11 H. H. Sønsteby, V. A.-L. K. Killi, T. A. Storaas, D. Choudhury, J. W. Elam, H. Fjellvåg, and O. Nilsen, *Dalton Trans.* **49**, 13233 (2020).
- 12 K. Huml, *Czech. J. Phys.* **15**, 699 (1965).
- 13 E. Østreg, H. H. Sønsteby, S. Øien, O. Nilsen, and H. Fjellvåg, *Dalton Trans.* **43**, 16666 (2014).
- 14 M. H. Chisholm, S. R. Drake, A. A. Naiini, and W. E. Streib, *Polyhedron* **10**, 337 (1991).
- 15 H. Nekola, F. Olbrich, and U. Behrens, *Z. Anorg. Allg. Chem.* **628**, 2067 (2002).
- 16 M. S. Bains, *Can. J. Chem.* **42**, 945 (1964).
- 17 H. H. Sønsteby, K. Weibye, J. E. Bratvold, and O. Nilsen, *Dalton Trans.* **46**, 16139 (2017).
- 18 H. H. Sønsteby, A. Yanguas-Gil, and J. W. Elam, *J. Vac. Sci. Technol. A* **38**, 020804 (2020).

- ¹⁹D. Caine and D. S. Roman, *Encyclopedia of Reagents for Organic Synthesis* (Wiley, Chichester, West Sussex, United Kingdom, 2009).
- ²⁰O. Nilsen, K. B. Gandrud, A. Ruud, and H. Fjellvåg, *Atomic Layer Deposition in Energy Conversion Applications* (Wiley, Weinheim, Germany, 2017).
- ²¹M. Putkonen, T. Aaltonen, M. Alnes, T. Sajavaara, O. Nilsen, and H. Fjellvåg, *J. Mater. Chem.* **19**, 8767 (2009).
- ²²E. Østeng, P. Vajeeston, O. Nilsen, and H. Fjellvåg, *RSC Adv.* **2**, 6315 (2012).
- ²³T. Aaltonen, M. Alnes, O. Nilsen, L. Costelle, and H. Fjellvåg, *J. Mater. Chem.* **20**, 2877 (2010).
- ²⁴N. Hornsveld, B. Put, W. M. M. Kessels, P. M. Vereecken, and M. Creatore, *RSC Adv.* **7**, 41359 (2017).
- ²⁵J. Xie *et al.*, *ACS Nano* **11**, 7019 (2017).
- ²⁶L. Chen *et al.*, *ACS Appl. Mater. Interfaces* **10**, 26972 (2018).
- ²⁷J. Kvalvik, K. B. Kvamme, K. Almaas, A. Ruud, H. H. Sonstebj, and O. Nilsen, *J. Vac. Sci. Technol. A* **38**, 050401 (2020).
- ²⁸T. Aaltonen, O. Nilsen, A. Magrasó, and H. Fjellvåg, *Chem. Mater.* **23**, 4669 (2011).
- ²⁹Y. Cao, X. Meng, and J. W. Elam, *ChemElectroChem* **3**, 858 (2016).
- ³⁰B. Wang, Y. Zhao, M. N. Banis, Q. Sun, K. R. Adair, R. Li, T.-K. Sham, and X. Sun, *ACS Appl. Mater. Interfaces* **10**, 1654 (2017).
- ³¹J. Hämäläinen, J. Holopainen, F. Munnik, T. Hatanpää, Mikko Heikkilä, Mikko Ritala, and M. Leskelä, *J. Electrochem. Soc.* **159**, A259 (2012).
- ³²B. Wang, J. Liu, M. N. Banis, Q. Sun, Y. Zhao, R. Li, T.-K. Sham, and X. Sun, *ACS Appl. Mater. Interfaces* **9**, 31786 (2017).
- ³³J. Liu, M. N. Banis, X. Li, A. Lushington, M. Cai, R. Li, T.-K. Sham, and X. Sun, *J. Phys. Chem. C* **117**, 20260 (2013).
- ³⁴V. Miikkulainen, O. Nilsen, M. Laitinen, T. Sajavaara, and H. Fjellvåg, *RSC Adv.* **3**, 7537 (2013).
- ³⁵Y.-C. Perng, J. Cho, S. Y. Sun, D. Membreno, N. Cirigliano, B. Dunn, and J. P. Chang, *J. Mater. Chem. A* **2**, 9566 (2014).
- ³⁶J. Liu, M. N. Banis, Q. Sun, A. Lushington, R. Li, T.-K. Sham, and X. Sun, *Adv. Mater.* **26**, 6472 (2014).
- ³⁷E. Kazyak, K.-H. Chen, K. N. Wood, A. L. Davis, T. Thompson, A. R. Bielinski, A. J. Sanchez, X. Wang, and C. Wang, *Chem. Mater.* **29**, 3785 (2017).
- ³⁸A. C. Kozen, A. J. Pearse, C.-F. Lin, M. Noked, and G. W. Rubloff, *Chem. Mater.* **27**, 5324 (2015).
- ³⁹M. Nisula, Y. Shindo, H. Koga, and M. Karppinen, *Chem. Mater.* **27**, 6987 (2015).
- ⁴⁰S. Shibata, *J. Electrochem. Soc.* **163**, A2555 (2016).
- ⁴¹B. Wang, J. Liu, Q. Sun, B. Xiao, R. Li, T.-K. Sham, and X. Sun, *Adv. Mater. Interfaces* **3**, 1600369 (2016).
- ⁴²A. S. Cavanagh, Y. Lee, B. Yoon, and S. George, *ECS Trans.* **33**, 223 (2010).
- ⁴³D. J. Comstock and J. W. Elam, *J. Phys. Chem. C* **117**, 1677 (2013).
- ⁴⁴J. Liu, M. N. Banis, B. Xiao, Q. Sun, A. Lushington, R. Li, J. Guo, T.-K. Sham, and X. Sun, *J. Mater. Chem. A* **3**, 24281 (2015).
- ⁴⁵D. J. Hagen and M. Karppinen, *J. Vac. Sci. Technol. A* **38**, 03241 (2020).
- ⁴⁶L. Egerton and D. M. Dillon, *J. Am. Ceram. Soc.* **42**, 438 (1959).
- ⁴⁷F. S. Chen, J. E. Geusic, S. K. Kurtz, J. G. Skinner, and S. H. Wemple, *J. Appl. Phys.* **37**, 388 (1966).
- ⁴⁸G. Popov, M. Mattinen, T. Hatanpää, M. Vehkamäki, M. Kemell, K. Mizohata, J. Räisänen, M. Ritala, and M. Leskelä, *Chem. Mater.* **31**, 1101 (2019).
- ⁴⁹A. I. Lebedev, *Phys. Solid State* **57**, 331 (2015).
- ⁵⁰Y. Wang *et al.*, *Science* **365**, 591 (2019).
- ⁵¹Y.-J. Dai, X.-W. Zhang, and K.-P. Chen, *Appl. Phys. Lett.* **94**, 042905 (2009).
- ⁵²M. Lie, O. Nilsen, H. Fjellvåg, and A. Kjekshus, *Dalton Trans.* **2009**, 481 (2009).
- ⁵³See supplementary material at <http://dx.doi.org/10.1116/6.0000589> for experimental details for deposition of Cs-containing thin films by ALD and detailed peak XPS spectra for Cs, Nb, O and C.
- ⁵⁴V. A.-L. K. Killi, "The role of passivation in deposition of thin films of K_xNbO_3 ," B.Sc. thesis, University of Oslo (2018).